



RESEARCH MEMORANDUM

TENSILE PROPERTIES OF SOME SHEET MATERIALS UNDER
RAPID-HEATING CONDITIONS

By George J. Heimerl and John E. Inge

Langley Aeronautical Laboratory
Langley Field, Va.

RECEIVED COPY

JUN 12 1955

LANGLEY AERONAUTICAL LABORATORY
WASHINGTON, D.C.
U.S. AIR FORCE

**NATIONAL ADVISORY COMMITTEE
FOR AERONAUTICS**

WASHINGTON

June 9, 1955

NACA RM L55E12b



NATIONAL ADVISORY COMMITTEE FOR AERONAUTICS

RESEARCH MEMORANDUM

TENSILE PROPERTIES OF SOME SHEET MATERIALS UNDER
RAPID-HEATING CONDITIONS

By George J. Heimerl and John E. Inge

SUMMARY

Results are presented of some rapid-heating tests of some sheet materials - 7075-T6 and 2024-T3 (formerly 75S-T6 and 24S-T3, respectively) aluminum alloys, Inconel, and RS-120 titanium alloy - which are part of an investigation of a number of structural materials. The materials were tested at temperature rates from 0.2° F to 100° F per second under constant-load conditions. Yield and rupture temperatures, obtained under rapid-heating conditions, are compared with the tensile properties obtained under constant-temperature conditions for 1/2-hour exposure. Yield and rupture stresses are found to increase approximately in proportion to the logarithm of the temperature rate except where effects such as aging altered the results. Master curves are presented for the determination of yield and rupture stresses and temperatures, which are based upon the use of a temperature-rate parameter derived from the data.

INTRODUCTION

Comparatively little is known about the properties of materials under rapid-heating conditions except for fairly recent tests of various materials by some investigators at temperature rates of hundreds of degrees or more per second (for example, refs. 1 to 5). This paper will cover some results of rapid-heating tests at relatively slow temperature rates up to 100° F per second for some sheet materials - 7075-T6 and 2024-T3 aluminum alloys, Inconel, and RS-120 titanium alloy - which are part of an investigation of a number of structural materials at the Langley Laboratory. The data on the latter two materials are preliminary. Detailed results for the two aluminum alloys are given in reference 6 along with a description of the equipment and test procedures.

The rapid-heating test is a new kind of test and differs from the conventional stress-strain test. In the rapid-heating test, the load is held constant. The material is then heated at a constant temperature rate until failure occurs. In the stress-strain test, on the other hand, the temperature is held constant. After the material has been heated 1/2 hour or more at the test temperature, the load is then applied until failure takes place. Heating was accomplished in the rapid-heating tests

by passing an electric current through the specimen in such a manner as to obtain a constant temperature rate. Autographic strain and temperature-time records were obtained, and yield and rupture temperatures were determined for each test.

TEST RESULTS

The strain-temperature histories for the tests of 7075-T6 aluminum alloy under rapid-heating conditions are shown in figure 1. In this figure the strains, which include the elastic, thermal, and plastic strains, are plotted against the instantaneous temperatures for each test at the different stress levels and temperature rates. These rates varied from about 0.2°F to 100°F per second - a factor of about 500. The outstanding characteristic of these tests for this material is the regular family of curves obtained at each stress level for the different temperature rates when the material becomes plastic. As long as the material remains elastic, however, a single curve is obtained at each stress level regardless of temperature rate. This single curve coincides with the calculated thermal-expansion and change-in-elastic-modulus curve for the stress level. The extensions of these calculated elastic curves are shown by the dashed lines. A thermal-expansion curve is also shown in figure 1 which was obtained for the material after it had been repeatedly heated and cooled until the same curve was obtained on both heating and cooling. Yield temperatures at which 0.2-percent plastic flow occur are indicated by the tick marks; yield temperatures increase with the temperature rate in a very consistent manner.

Figure 2 shows the logarithmic nature of this increase in yield as well as in rupture temperatures for this material. The temperature rate is given by a logarithmic scale. The curves are faired through the test points and show that both yield and rupture temperatures increase approximately in proportion to the logarithm of the temperature rate. This condition was also found to be the case for the other materials with certain specific exceptions, some of which will now be illustrated.

Figure 3 shows the effect of aging on the results for 2024-T3 aluminum alloy at 50 ksi. In this instance, all the test curves go more or less together up to yield, after which the individual curves fall into the normal pattern. Rupture temperatures follow a logarithmic relation but yield temperatures do not.

Another example of the effect of aging is shown in figure 4 for RS-120 titanium alloy at 75 ksi. In this case, the test results follow the usual pattern up to yield, but at higher temperatures the order of the curves is almost completely reversed. This behavior was not expected for this material in the stabilized annealed condition.

The last example (fig. 5) illustrates the unstable nature of the plastic flow obtained in the tests of Inconel at 28 ksi under rapid-heating conditions. Here, abrupt plastic flow occurs after intervals of more or less elastic action. In spite of this erratic behavior, yield temperatures appear to increase in regular fashion; this irregular behavior continued until near rupture. This type of action is associated with the development of Lüders' lines.

COMPARISON OF RAPID-HEATING AND STRESS-STRAIN TESTS

Although rapid-heating and stress-strain tests are two distinctly different kinds of tests, comparisons can be made between results of such tests on the basis of yield and rupture or ultimate stresses at different temperatures. The comparative results for the yield stress for the aluminum alloys are shown in figure 6. The results of the rapid-heating tests are given by the solid lines for arbitrary temperature rates from 0.2° F to 100° F per second. The dashed lines give the tensile yield stress (0.2-percent offset) for 1/2-hour exposure obtained from the stress-strain test. The main result to be noted here is that the yield stress under rapid-heating conditions may be appreciably greater or about the same at a given temperature as that obtained from the stress-strain test for 1/2-hour exposure, depending on the temperature rate and the material. For the rapid-heating tests, the effect of increase in temperature rate levels off markedly for rates above about 60° F per second.

A comparison of the rapid-heating and stress-strain results for these same materials for rupture and ultimate stress is given in figure 7. The comparisons are very similar to those found for the yield shown in figure 6. Rupture temperatures, however, run from 20° F to 60° F higher than those for yield. As in the case of yield, the increase in rupture stress becomes very small for temperature rates above 60° F to 100° F per second. Similar comparisons between rapid-heating and tensile-test results for Inconel and RS-120 titanium alloy have not been completed.

MASTER YIELD AND RUPTURE CURVES

A temperature-rate parameter was derived from the data, which was based upon the logarithmic relationship between yield and rupture temperatures and the temperature rate previously shown. With this parameter, it was found possible to reduce the results of the rapid-heating tests to a single or master curve in plots of stress against the parameter.

The correlation of the data with the master curves for the two aluminum alloys is shown in figure 8. In this parameter, T applies either to the yield or rupture temperature in $^{\circ}\text{F}$, and h is the temperature rate in $^{\circ}\text{F}$ per second; the additional numbers in the numerator and denominator are temperature and temperature-rate constants, respectively. The validity of the parameter is shown by the correlation of the data with the master curves. Very good correlations were obtained in general for yield for both materials and fairly good correlation for rupture. Yield and rupture temperatures, calculated by means of the master curve and the parameter for the different stress levels, are in very close agreement with the test values, especially for the 7075-T6 aluminum alloy.

Figure 9 shows the correlation of the test points with the master curves for yield and rupture for Inconel and RS-120 titanium alloy. Good correlations were obtained for yield for Inconel and the titanium alloy except at 50 ksi for the latter where the parameter does not hold. Fairly good correlation was obtained for rupture for these materials except in the regions where aging affected the results.

CONCLUDING REMARKS

Although the rapid-heating tests for some of the materials have not been completed, the results obtained so far indicate, in general, that yield and rupture temperatures increase logarithmically with temperature rates below 100°F per second except for certain regions or stress levels for some of the materials. This increase levels off markedly for temperature rates from about 60°F to 100°F per second. Under rapid-heating conditions, materials may be stronger than indicated by conventional tensile data for 1/2-hour exposure, but the relative strength varies with the temperature rate and the material. At the present time, no theory is available for the complex transient behavior of materials under rapid-heating conditions. The use of master yield and rupture curves, however, employing a suitable temperature-rate parameter, affords a possible convenient method for determining yield and rupture stresses and temperatures for different temperature rates. In any case, adequate data are required for each material in order to establish such curves and the limitations of the parameter.

Langley Aeronautical Laboratory,
National Advisory Committee for Aeronautics,
Langley Field, Va., April 25, 1955.

REFERENCES

1. Cross, H. C., McMaster, R. C., Simmons, W. F., and VanEcho, J. A.: Short-Time, High-Temperature Properties of Heat-Resisting Alloy Sheet. Project RAND (USAF Project MX-791) RA-15077, Douglas Aircraft Company, Inc., Feb. 27, 1948.
2. Smith, W. K., Wetmore, W. O., and Woolsey, C. C., Jr.: Tensile Properties of Metals While Being Heated at High Rates. NAVORD Rep. 1178, Pt. 1 (NOTS 234), U. S. Naval Ord. Test Station (Inyokern, Calif.), Sept. 7, 1949.
3. Smith, W. K., Woolsey, C. C., Jr., and Wetmore, W. O.: Tensile Properties of Metals While Being Heated at High Rates. Pt. 2 - Aluminum Alloys. NAVORD Rep. 1178 (NOTS 319), U. S. Naval Ord. Test Station, Inyokern (China Lake, Calif.), Sept. 1, 1950.
4. Smith, W. K., Woolsey, C. C., Jr., and Wetmore, W. O.: Tensile Properties of Metals While Being Heated at High Rates. Pt. 3 - Comparison of Results From High-Heating-Rate Tests With Results From Rocket Firing Tests. NAVORD Rep. 1178 (NOTS 336), U. S. Naval Ord. Test Station, Inyokern (China Lake, Calif.), Dec. 20, 1950.
5. Smith, W. K.: High-Heating-Rate Strength of Titanium and Two Titanium Alloys. NAVORD Rep. 1958 (NOTS 526), U. S. Naval Ord. Test Station, Inyokern (China Lake, Calif.), Apr. 10, 1952.
6. Heimerl, George J., and Inge, John E.: Tensile Properties of 7075-T6 and 2024-T3 Aluminum-Alloy Sheet Heated at Uniform Temperature Rates Under Constant Load. NACA TN 3462, 1955.

STRAIN-TEMPERATURE CURVES FOR 7075-T6 ALUMINUM ALLOY

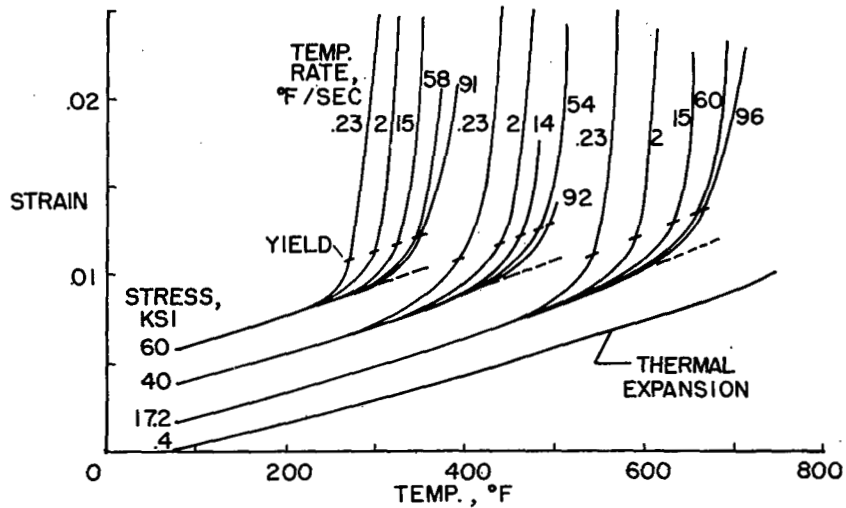


Figure 1

YIELD AND RUPTURE TEMP. FOR 7075-T6

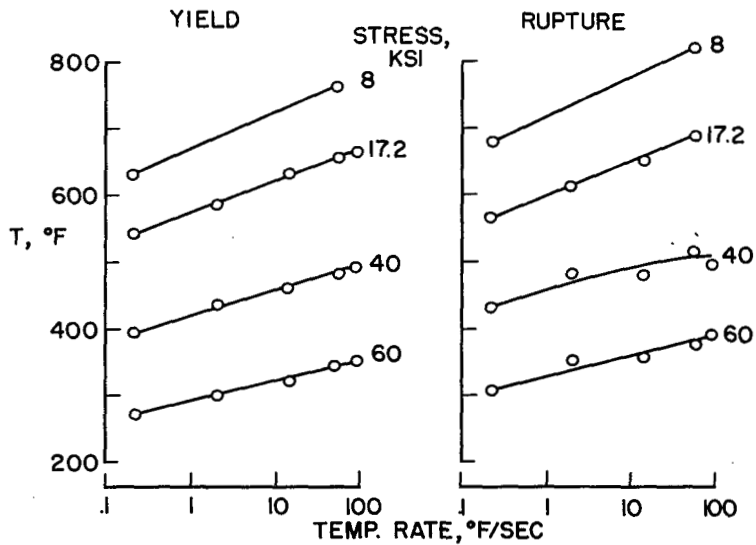


Figure 2

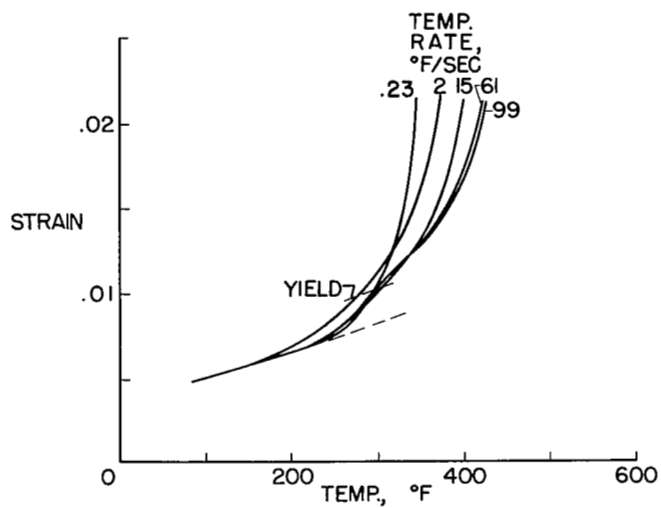
AGING OF 2024-T3 ALUMINUM ALLOY
AT 50 KSI

Figure 3

AGING OF RS-120 TITANIUM ALLOY AT 75 KSI

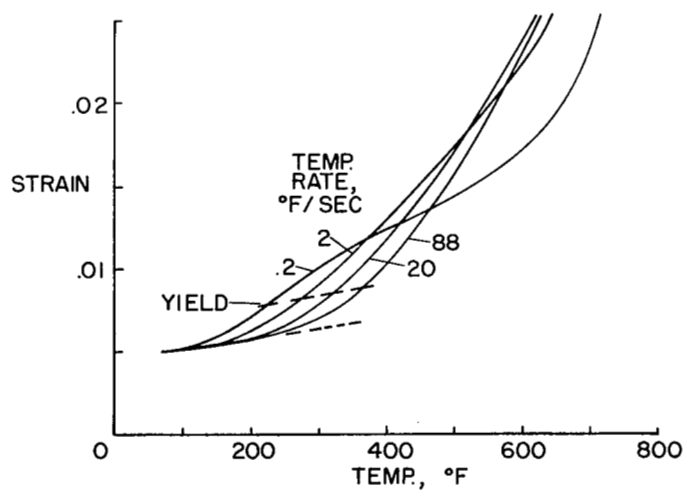


Figure 4

UNSTABLE PLASTIC FLOW OF INCONEL AT 28 KSI

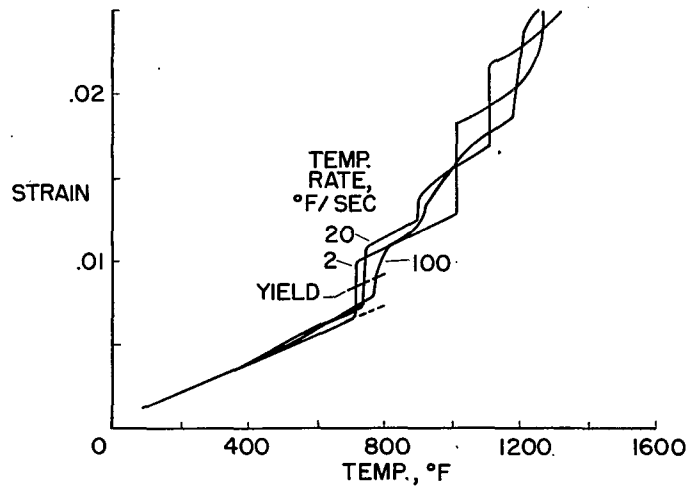


Figure 5

COMPARISON OF RAPID-HEATING AND STRESS-STRAIN RESULTS FOR YIELD

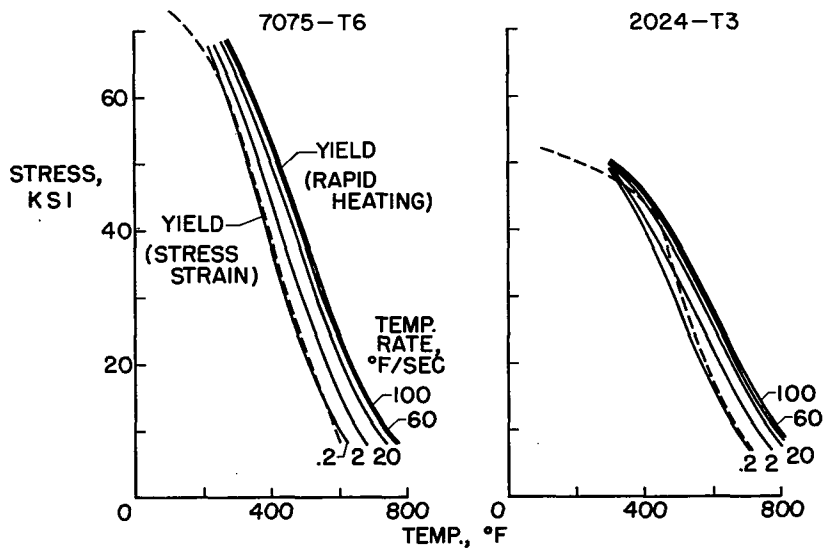


Figure 6

COMPARISON OF RAPID-HEATING AND STRESS-STRAIN RESULTS FOR RUPTURE AND ULTIMATE

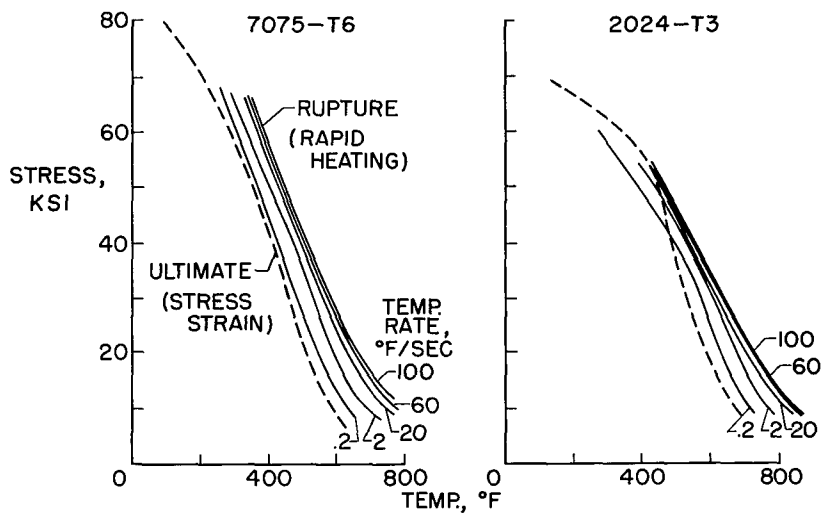


Figure 7

MASTER CURVES FOR YIELD AND RUPTURE

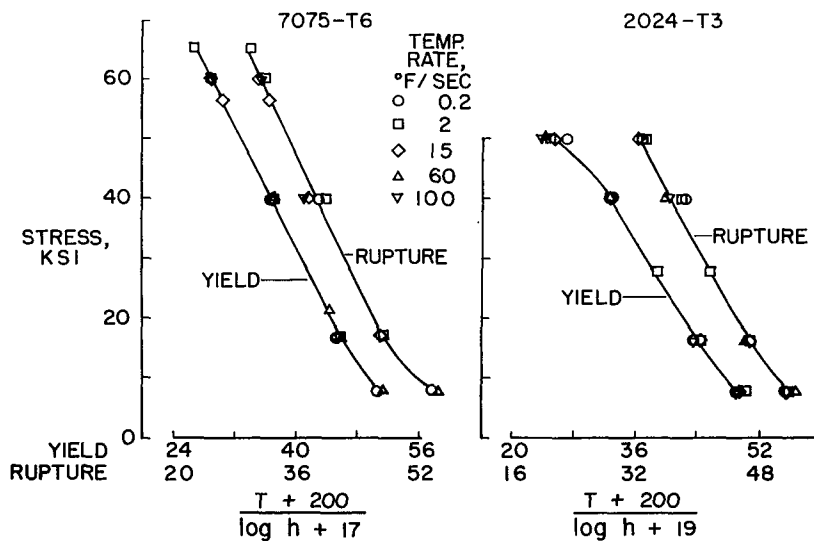


Figure 8

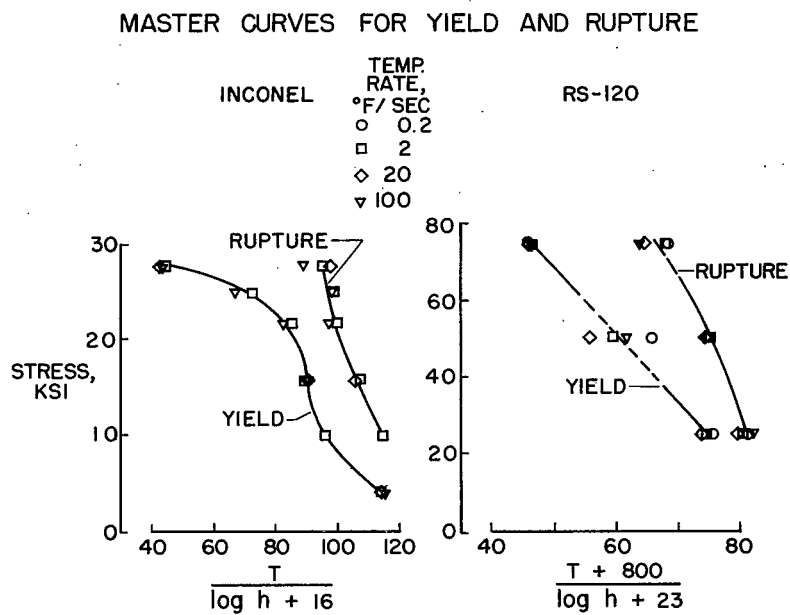
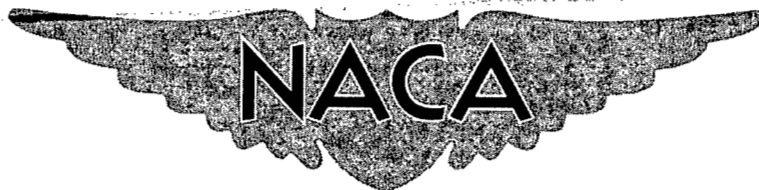


Figure 9

NASA Technical Library



3 1176 01437 6850



RESEARCH MEMORANDUM

SUMMARY OF RECENT THEORETICAL AND EXPERIMENTAL
WORK ON BOX-BEAM VIBRATIONS

By John M. Hedgepeth

Langley Aeronautical Laboratory
Langley Field, Va.

NATIONAL ADVISORY COMMITTEE
FOR AERONAUTICS

WASHINGTON

June 14, 1955



NATIONAL ADVISORY COMMITTEE FOR AERONAUTICS

RESEARCH MEMORANDUM

SUMMARY OF RECENT THEORETICAL AND EXPERIMENTAL

WORK ON BOX-BEAM VIBRATIONS

By John M. Hedgepeth

SUMMARY

A discussion of various secondary effects which have an important influence on the vibration characteristics of box beams is presented. Means of incorporating these effects in vibration analyses of actual built-up box beams are discussed. Comparisons with experiment are given; good agreement between theory and experiment is obtained when the secondary effects are included.

INTRODUCTION

The need of accurate vibration modes and frequencies of aircraft is well recognized. The reliability of a flutter-speed calculation, for example, is intimately related to the accuracy of the vibration modes and frequencies - especially the frequencies - used in the analysis. Furthermore, these modes and frequencies are often useful in the analysis of other dynamic problems, such as landing impact and gust loads.

The purpose of this paper is to summarize the results of research into the vibration characteristics of one of the main types of aircraft structures - the box beam. Most of the information to be discussed is recent; some of it is old and is included in order to present a complete story.

DISCUSSION

Shown in figure 1 is a drawing of a typical box beam which may be thought of as being the main load-carrying structure of a wing. It is composed of covers built up of sheet stiffened by stringers, and spars made up of flanges connected by webs. There are usually a number of ribs to provide cross-sectional stiffness.

The vibration analyses of beams like the one shown in figure 1 ordinarily have used elementary beam bending and torsion theory. The accuracy obtained from elementary theory was considered to be good enough for long beams. However, it is known that, in the deformation of box beams, certain secondary effects arise which are not taken into account in the elementary theory. These secondary effects can have an important influence on the vibration characteristics of box beams, particularly when the higher modes are desired.

In bending vibrations, the secondary effects that are generally recognized are transverse shear, shear lag, and longitudinal (rotary) inertia. Transverse shear arises from the fact that shear deflections of the box occur under load because of the finite shear stiffness of the webs. These shear deflections are in addition to the bending deflections considered in the elementary theory. Shear lag is caused by the finite shear stiffness of the covers which permits the direct-stress-carrying material in the middle of the cover to carry less than its full share of the load. Both of these effects tend to reduce the apparent stiffness of the box and, hence, to reduce the natural frequencies. Longitudinal inertia arises from the fact that, when the beam vibrates, inertia forces are developed because of accelerations in the longitudinal direction. This effect - which is often called rotary inertia in the bending problem - is of course not included in the elementary theory and tends to reduce the natural frequencies.

The quantitative influence of these effects on the bending frequencies of vibration of uniform, thin-walled box beams was investigated by Budiansky and Kruszewski (ref. 1). Reference 1 shows that the effects of transverse shear and shear lag are of comparable magnitude and can be quite important, particularly for short beams. On the other hand, the effect of longitudinal inertia is negligible for the shallow box beams that are typical of aircraft wing construction.

For torsional vibrations, the secondary effects that are generally recognized are restraint of warping and longitudinal inertia. When a beam is twisted, the cross sections tend to distort out of their own plane or to warp. In the elementary theory, this warping is allowed to occur without restraint. However, if the warping varies along the length, as it does in a vibration mode, direct stresses are created in the longitudinal direction which act to restrain the warping. The effect of this restraint of warping is to make the beam stiffer than it would be otherwise and, consequently, to raise the natural frequency. This warping motion also causes inertia forces in the longitudinal direction. This longitudinal inertia effect is not included in the elementary theory.

The quantitative influence of these secondary effects on the torsional frequencies of uniform, thin-walled box beams was investigated

by Kruszewski and Kordes (ref. 2). Reference 2 shows that the effect of restraint of warping could be appreciable for short beams although the effects are not so pronounced as those incurred in the bending case. The effect of longitudinal inertia was unimportant for practical box beams.

Before considering the influence of these secondary effects on the bending and torsion frequencies of some actual test specimens, it is desirable to discuss how the effects of transverse shear, shear lag, and restraint of warping can be incorporated in vibration analyses of actual box beams. The results in references 1 and 2 were obtained for highly idealized beams for which exact solutions were possible. In an actual box beam, exact solutions are not feasible and some sort of simplified structure must be used.

The cross section of the box beam shown in figure 2 contains a large number of elements - stringers, flanges, and the sheet joining them. If all of these elements were treated separately in an analysis, the calculation job would be overwhelming. By lumping the properties of these elements, however, the effects of transverse shear and shear lag can be obtained without an inordinate amount of labor. The transverse-shear effect can be included simply by allowing the webs to have shear flexibility. The shear-lag effect can be duplicated by using the substitute-stringer idealization shown in figure 2. The direct-stress-carrying areas in the webs and flanges are concentrated at the corners; the direct-stress-carrying areas in the covers are concentrated as so-called substitute stringers. By properly locating the substitute stringers, it is possible to obtain frequencies within a couple of percent of those predicted by more refined theories. The use of the substitute-stringer idealization has been investigated in reference 3. For the torsion problem, the so-called four-flange box is useful in obtaining frequencies. In this idealization the direct-stress-carrying areas in both the covers and the webs are concentrated at the corners. The four-flange box does a good job of duplicating the effect of restrained warping on torsional vibrations. It might be mentioned that the substitute-stringer box can also be used for torsional vibrations with comparable success. This is fortunate since, in most actual box beams, bending and torsion will couple and the idealization used should be capable of taking all secondary effects into account.

Simplifying the cross section of the box beam is only part of what is necessary to achieve a practical vibration analysis. For a non-uniform box beam, further simplifications must be made as to the behavior in the spanwise direction. One approach is to break up the beam into a number of bays and to calculate influence coefficients. These influence coefficients then provide a basis for the vibration analysis. (See, for example, ref. 4.) Calculations have been made to

determine the number of bays necessary to obtain accurate frequencies. The results indicate that, in order to obtain the first three symmetrical bending and torsion frequencies of a free-free box beam, it is necessary to use about eight bays on the half span.

An experimental vibration-test investigation has been conducted in order to check the accuracy of methods of computing natural modes and frequencies. Tests have been carried out on two structures - one a large-scale built-up box beam and the other a somewhat smaller, hollow rectangular tube.

Consider first the built-up box beam. In figure 3 is shown a photograph of the vibration-test setup used to determine its natural modes and frequencies experimentally. The beam was 20 feet long, 18 inches wide, and 5 inches deep. The aspect ratio was about 13. The beam was hung from the gallows and was vibrated horizontally. In this way an essentially free-free condition was attained. The beam was vibrated by means of four electromagnetic shakers attached at the corners. Power was supplied by the M-G set and controlled at the left-hand cabinet in figure 3. Pickups were mounted on the beam and were used to sense the motion; their output was recorded at the right-hand cabinet.

The vibration frequencies of this beam are given in table I. In the table, for simplicity, only symmetrical bending frequencies and antisymmetrical torsion frequencies have been shown; the antisymmetrical bending and symmetrical torsion frequencies follow the same trends. For both the bending and torsion, the frequencies in the first column were obtained experimentally; the frequencies in the second column were calculated by elementary theory. The frequencies including the secondary effects are given in the last column. The word "exact" has been used for these frequencies for want of a better term. By comparing experiment and elementary theory, it can be seen that the elementary theory is accurate enough for the torsion modes and for the first bending mode. For the higher bending modes, however, the situation is different. Errors varying from 20 percent in the second mode to 70 percent in the fourth mode are experienced. When the secondary effects are included, however, the agreement is considerably improved. By looking at the bending modes, it can be seen that the large reductions in frequency due to transverse shear and shear lag have brought the calculations into satisfactory agreement with the experiment. It might be mentioned that transverse shear and shear lag were about equally responsible for this reduction. For the torsion modes, inclusion of the smaller effect of restraint of warping has helped for the first two modes and hurt for the third. Even for this third antisymmetrical torsion mode - which is the twelfth mode of the beam - the error is only 6 percent.

The built-up box beam which has been discussed had a large amount of internal stiffening in the form of stringers and bulkheads. The other

specimen - a hollow rectangular tube - was considerably simpler and was tested for the purpose of checking theories before the vibration equipment necessary for testing large-scale built-up structures was obtained. The results for this hollow rectangular tube which is shown in figure 4 serve to illustrate an effect which may be important for box beams with little internal stiffening. This tube was approximately 8 feet long, 7 inches wide, and 2 inches deep. The aspect ratio was about 14. It was made by welding 1/4-inch plates together along the corners.

The results of vibration tests are given in table II. Again in this table only the symmetrical bending frequencies and antisymmetrical torsion frequencies are presented. Along with the experimental frequencies are given the "exact" calculated frequencies for which the secondary effects of transverse shear, shear lag, and restraint of warping have been included. For the first two symmetrical bending modes, the "exact" frequencies are fairly good; for the rest of the modes shown here, however, the errors are large - especially for the torsion modes. The reason for these large discrepancies is tied up with the occurrence of large cross-sectional distortions which were not taken into account in the calculations. The nature of these distortions is illustrated in figure 5.

When a box is undergoing a bending vibration, the inertia forces tend to bend the covers and webs in a manner like that shown at the top of figure 5. This distortion, in turn, causes additional inertia forces which tend to raise the effective mass of the beam and lower the frequency. For torsional vibrations there occurs a similar bending of the webs and covers. More importantly, however, the cross section undergoes an overall shear. Both of these effects tend to raise the effective mass moment of inertia and, hence, to lower the torsional frequencies. In an ordinary box, the presence of stiffening members, such as stringers and ribs or bulkheads, tends to prevent these cross-sectional distortions. In the tube, however, there were no such stiffeners, and the frequencies were therefore greatly reduced.

It should be mentioned that one of the present trends in structural design is in the direction of eliminating stringers and bulkheads and letting the skin carry most of the load. Therefore, this effect of cross-sectional flexibility may indeed become important for actual box beams, just as it is for the hollow tube.

Studies of the effects of cross-sectional distortions on the bending and torsional frequencies of box beams have been carried out. The effect of the local bending of the covers and webs has been presented in reference 5; an analysis of the effect of the overall shear of the cross-section has also been performed. Results of applying the corrections indicated by these studies to the frequencies of the hollow tube are shown by the frequencies in the last column of table II for both

symmetrical bending and antisymmetrical torsion. The agreement with experiment is now satisfactory for all the bending modes. The agreement for the torsional modes is surprisingly good considering the large effects taken into account by the approximate correction.

CONCLUDING REMARKS

From the comparisons between theory and experiment that have been discussed for the box beams, it can be concluded that the secondary effects of transverse shear and shear lag can have an important influence on the bending vibrations of box beams. This is true even for long beams if the higher modes are desired. The effect of restraint of warping on the torsional modes is not nearly so important. The effects of cross-sectional distortion can be quite large unless stiffening members are used to minimize the distortion. In any event, the methods developed for taking all these effects into account are very successful.

Langley Aeronautical Laboratory,
National Advisory Committee for Aeronautics,
Langley Field, Va., April 22, 1955.

REFERENCES

1. Budiansky, Bernard, and Kruszewski, Edwin T.: Transverse Vibration of Hollow Thin-Walled Cylindrical Beams. NACA Rep. 1129, 1953. (Supersedes NACA TN 2682.)
2. Kruszewski, Edwin T., and Kordes, Eldon E.: Torsional Vibrations of Hollow Thin-Walled Cylindrical Beams. NACA TN 3206, 1954.
3. Davenport, William W., and Kruszewski, Edwin T.: A Substitute-Stringer Approach for Including Shear-Lag Effects in Box-Beam Vibrations. NACA TN 3158, 1954.
4. Levy, Samuel: Computation of Influence Coefficients for Aircraft Structures With Discontinuities and Sweepback. Jour. Aero. Sci., vol. 14, no. 10, Oct. 1947, pp. 547-560.
5. Budiansky, Bernard, and Fralich, Robert W.: Effects of Panel Flexibility on Natural Vibration Frequencies of Box Beams. NACA TN 3070, 1954.

TABLE I
FREQUENCIES OF BUILT-UP BOX

<u>SYMMETRICAL BENDING</u>				<u>ANTISYMMETRICAL TORSION</u>			
MODE	EXP, CPS	ELEM., CPS	"EXACT", CPS	MODE	EXP, CPS	ELEM., CPS	"EXACT", CPS
1	18.1	18.4	18.0	1	64.7	63.0	63.3
2	84.7	101.0	86.4	2	194.0	189.0	194.0
3	176.0	247.0	181.0	3	313.0	315.0	332.0
4	271.0	458.0	285.0				

TABLE II
FREQUENCIES OF HOLLOW TUBE

<u>SYMMETRICAL BENDING</u>				<u>ANTISYMMETRICAL TORSION</u>			
MODE	EXP, CPS	"EXACT", CPS	CORR., CPS	MODE	EXP, CPS	"EXACT", CPS	CORR., CPS
1	68.7	70.2	70.2	1	301.0	377.0	316.0
2	342.0	348.0	328.0	2	455.0	1133.0	485.0
3	572.0	761.0	586.0	3	648.0	1911.0	705.0

TYPICAL BOX BEAM

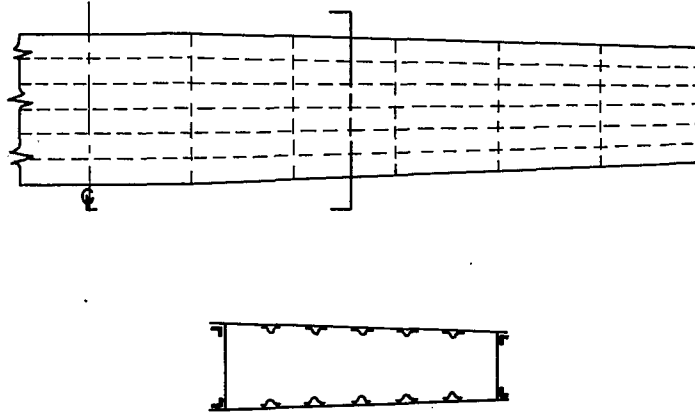


Figure 1

CROSS-SECTIONAL IDEALIZATIONS

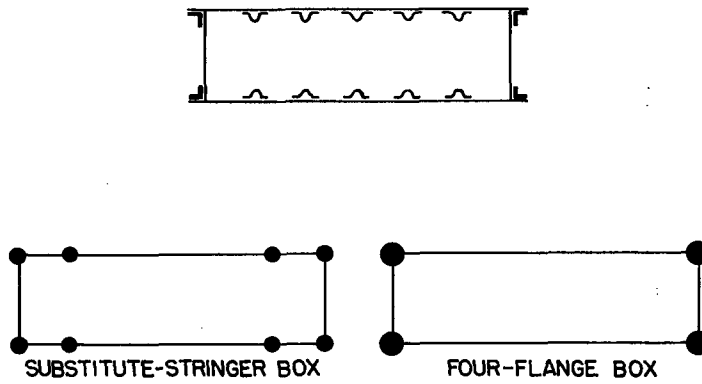


Figure 2

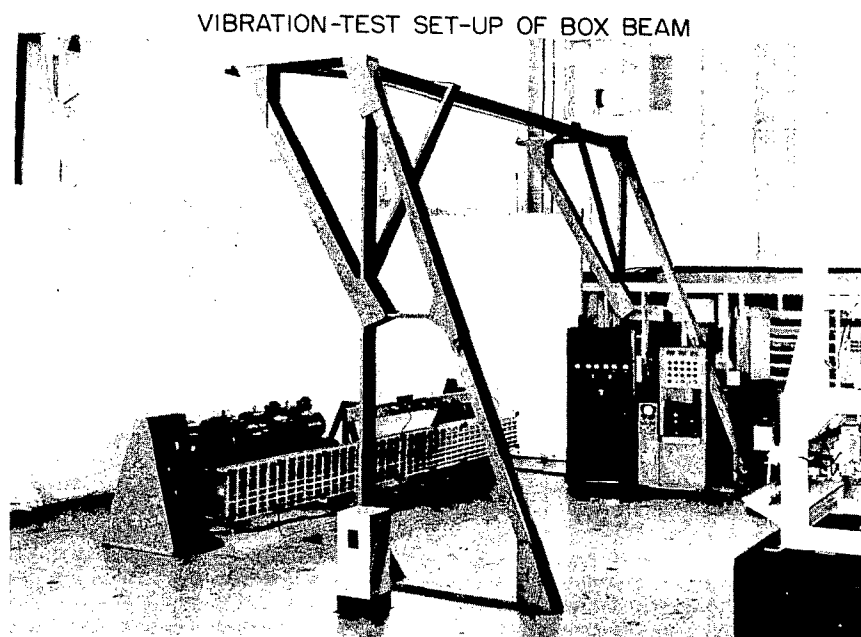


Figure 3

HOLLOW RECTANGULAR TUBE

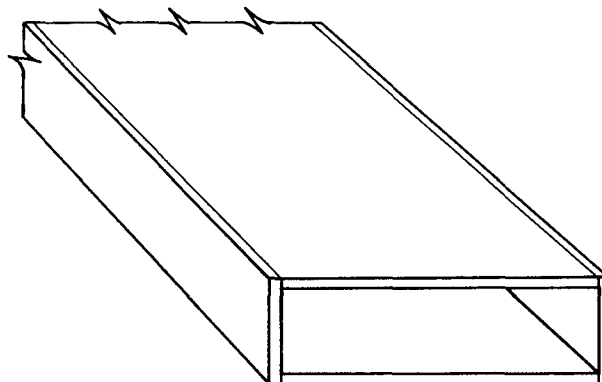


Figure 4

CROSS-SECTIONAL DISTORTIONS



BENDING



TORSION

Figure 5

1. The first part of the document is a list of the names of the persons who have been appointed to the various offices of the city of New York.

2.

3.

4.

5.

6.

7.

8.

9.

10.

11.

12.

13.

14.

15.

16.

17.

18.

19.

20.

21.

22.

23.

24.



3 1176 01437 6892